Part II. Chlorination of Sulfur Dioxide

The photochemical chlorination of sulfur dioxide was investigated experimentally. The photochemical reactor was the vortex-stabilized arc radiation source described in Part I. Aqueous inorganic solutions, providing selective wavelength filtration, were circulated through the inner annular region. The outer annulus served as the reaction volume. The dependence of the reaction on wavelength, reaction gas inlet temperature, pressure, and reactant flow rate was investigated. The amount of sulfur dioxide in the mixture was varied from 1/6 to 2/3 atmosphere. The photochemical rate of formation of sulfuryl chloride is best described by the rate expression:

$$r = J - k_0 \exp\left[-\frac{E}{RT}\sqrt{J/(SO_2)} \right] \cdot (SO_2Cl_2)$$

where J is the volumetric rate of light absorption and where k_0 and E have values of 0.0542 $s^{1/2}$ and −2.6 kcal/gmol, respectively.

SURVEY OF PREVIOUS WORK

The photochemical formation of sulfuryl chloride was investigated by Schumacher and Schott (1942) at 2° and 30°C. The investigations were performed according to a statistical method in a quartz container. Their light source had a spectral output centered between 3500 and 4500Å with the peak intensity located at approximately 4000Å. The reaction is strongly influenced by the wall which makes it difficult to reproduce the experiments.

The photochemical decomposition of sulfuryl chloride was also investigated by Schumacher and Schott (1942) at 110° and 130°C. Gas phase mixtures of sulfuryl chloride, sulfur dioxide, and chlorine were exposed to radiation from the 4360, 4050, and 3650Å mercury lines, which are absorbed only by chlorine. The overall reaction was believed to be a chain reaction proceeding according to the rate expression

$$r = -k\sqrt{\frac{J}{(SO_2)P}} \cdot (SO_2Cl_2) \qquad (1)$$

where J is the intensity of the absorbed radiation, P is the total pressure, and k is a rate constant having values of $(15 \pm 1) \times 10^{-3}$ and $(50 \pm 1) \times 10^{-3}$ mm of mercury/min. at 110 and 130°C, respectively. The temperature coefficient for a 10°C rise in temperature was 1.83 which indicates an apparent activation energy of 18 kcal/gmol.

Londergan (1942) studied the photochemical chlorination of SO_2 at 70°C in a pyrex reaction vessel with a circulating gas mixture. The quantum yield was observed to be 1.2 ± 0.2 for 4358Å light. The reaction velocity was first order with respect to the chlorine concentration.

An approximate value of 1.0 for the quantum yield was given by Bonhoeffer (1923) who used light with a wavelength of approximately 4200Å for the determination.

LeBlanc et al. (1919) manometrically studied the reaction at generally low initial pressures and at 55°, 105°, and 125°C. The temperature dependence of the formation reaction, using light that was only absorbed by chlorine, was low. The authors suggested that the reaction velocity depended on a small water vapor content.

Trautz (1915) measured the rate of formation of sulfuryl chloride in a quartz container at 291 and 372 K and at various concentrations. The reaction was observed to proceed via a second order mechanism. A temperature increase of 80 K lowered the reaction rate according to a coefficient of 0.88 for a 10 K increase in temperature.

Investigators of the photochlorination reaction tend to contradict each other on several points. For example, Schumacher and Schott (1942) state that the formation reaction is independent of the chlorine concentration while sulfur dioxide has an accelerating effect. Londergan (1942) reports that the reaction is first order with respect to the chlorine concentration. A third researcher, Trautz (1915), reports that the reaction is first order in both chlorine and sulfur dioxide. These and other anomalies among the various sets of data presented, involving the effects of such parameters as water vapor concentration, wall surface area, and temperature made this reaction a candidate for further study.

REACTION SYSTEM

The experimental system used in this investigation consisted of a plasma light source, an argon delivery system, a cooling water system, a dye solution circulation system, reactant delivery systems, a safety interlock system, and ultraviolet spectrographic analysis system, and an infrared spectrographic analysis system. A schematic diagram of this apparatus is presented in Figure 1 of Part I.

The reactor is shown schematically in Figure 2 of Part I. It consisted of an arc radiation source and an annular triple-walled quartz reaction vessel aligned on a common axis. Water soluble inorganic dyes, which provided selective wavelength filtration and process cooling, were circulated in the inner annulus. The outer annulus served as the reaction volume. Details of the operation of this reactor are discussed in Part I.

In preparation for an experimental run a glass sample tube was placed in the product gas stream in parallel with a bypass line. During the run the product stream was diverted from the bypass line, the sample tube was flushed, and a sample of product gas was obtained. Using a gas manifold system, part of the gas sample was transferred to a 5-cm path length infrared cell equipped with sodium chloride windows. An infrared spectrogram of the gas sample was then made using a recording infrared spectrophotometer. The infrared spectrogram was analyzed by comparing the strength of the sulfuryl chloride absorption peak at 7.06 μ with the strength of the sulfur dioxide absorption peak at 4.00 μ.

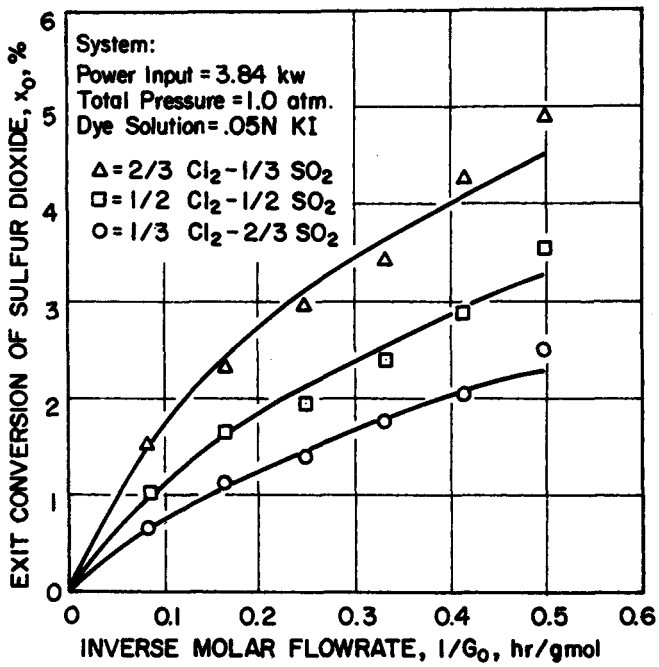

Fig. 1. Comparison of experimental data and predicted curves for several reactant mixtures while using KI dye solution.

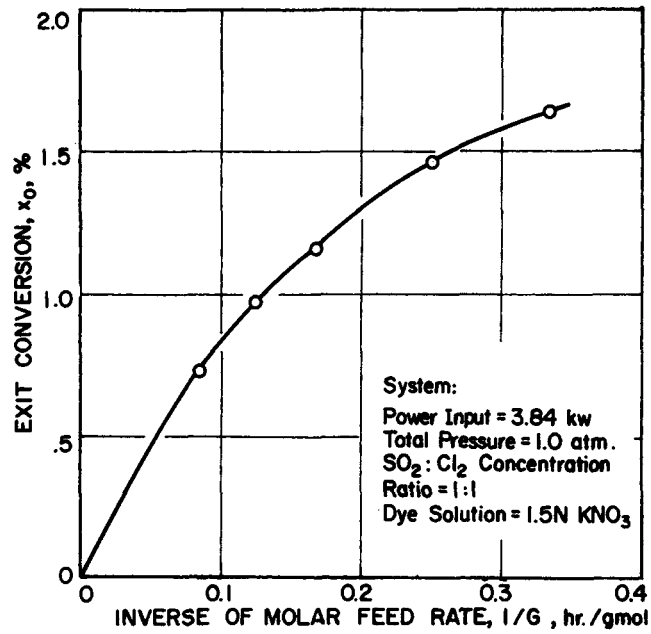

Fig. 2. Exit conversion of sulfur dioxide vs. the inverse of the molar feed rate.

QUANTITATIVE ANALYSIS

The experimentally determined values of exit conversion versus the inverse of the molar flow rate, as a function of the controllable parameters, were analyzed using a numerical method. This is necessary because of strong axial intensity variations.

The mole balance is [see Equation (13), Part I]

$$\frac{dx}{dz} = \frac{(1+a)A}{G_0} r \tag{2}$$

The energy balance is [see Equation (15), Part I]

$$\frac{G_0}{(1+a)}\left[c_{p_{SO_2}}(1-x) + c_{p_{Cl_2}}(a-x) + c_{p_{SO_2Cl_2}} \cdot x\right] \frac{dT}{dz} + \left(\frac{G_0 T}{(1+a)}\right) \cdot \left[-c_{p_{SO_2}} - c_{p_{Cl_2}} + c_{p_{SO_2Cl_2}}\right] \frac{dx}{dz} = r\Delta H_r A + WA - U\bar{A}(T - T_0) \tag{3}$$

The expression for dx/dz obtained above can be substituted into the second term of this equation.

In addition

$$\Delta H_r >> \left[-c_{p_{SO_2}} - c_{p_{Cl_2}} + c_{p_{SO_2Cl_2}}\right] T \tag{4}$$

so this term can be eliminated from consideration and the energy equation can be written

$$\frac{G_0}{(1+a)}\left[(1-x)c_{p_{SO_2}} + (a-x)c_{p_{Cl_2}} + xc_{p_{SO_2Cl_2}}\right] \frac{dT}{dz} = r\Delta H_r A + WA = U\bar{A}(T - T_0) \tag{5}$$

Assuming a functional form for the rate of reaction r:

$$r = r(x, z, T, a, G_0, J, \lambda) \tag{6}$$

for specific values of parameters such as G_0, a, and U, distributions of W and light intensity along the reactor length, it is possible to simultaneously integrate the mole balance and energy equations over the length of the reactor. Such an integration yields values of exit conversion versus the inverse of the molar flow rate, which may be compared with the experimental data for all combinations of the controllable parameters.

The distribution of the rate of heat generation due to light absorption and the rate of light absorption along the length of the reactor were predicted numerically using a digital computer and the results of Part I.

The distribution of light intensity along the reactor length was calculated from measured values of the spectral radiance of the arc.

The rate expression which gave the best agreement with the experimentally determined exit conversion versus the inverse of the molar flow rate for all combinations of controllable parameters was

$$r = \Phi J - k_0 \exp\left\{-\frac{E}{RT}\right\} (SO_2Cl_2) \sqrt{J/(SO_2)} \tag{7}$$

The quantum yield for the forward reaction was taken as 1.0 gmol/einstein based on this and previously mentioned work. In order to determine the values of the parameters E and k_0 found in the rate expression and the value of U found in the energy equation, a nonlinear regression analysis was performed on part of the data. The parameter E was calculated to be -2.6 kcal/gmol while k_0 was found to be 0.0542 $s^{-1/2}$. The value of the overall heat transfer coefficient U was observed to be small. The best agreement with the experimental data was obtained when U was assumed to be zero, that is, when the reaction was assumed to occur adiabatically. Because of the cooling effect of the dye solution, the reaction also occurred nearly isothermally. Only a 2° to 4°C temperature rise was noted in the runs.

The values given above are considered valid over the range of flow rates shown in Figure 1. Power to the arc was fixed at 3.84 kw for the kinetic studies, but power variations should result in only light intensity changes if cooling is efficient. Hence, no unusual changes would be expected at other power levels.

In Figure 1 the above rate expression, together with the mole balance and energy equations, was used to predict the experimental curves obtained for the various

combinations of the controllable parameters. It should be noted that the data shown in Figure 1 was not used in the nonlinear regression analysis.

DIFFERENTIAL REACTOR ANALYSIS

The reaction system used in this investigation was an adiabatic annular flow reactor with a nonconstant light flux along its length. Such a system typically presents some difficulty in the presentation of experimental observations. For purposes of qualitative analysis it is of value to develop a logical method for the graphical presentation of experimental observations.

The computer data analysis suggested the rate expression for the photochemical reaction given in Equation (7). That rate equation may be used in a mole balance in terms of the mole percent conversion of sulfur dioxide X and linear position along the reactor z:

$$\frac{G_0}{A(1+a)}\left(\frac{dX}{dz}\right)_{G_0} = J - k\sqrt{\frac{J \cdot P}{RT(1+a-X)\cdot(1-X)}}\,X \quad (8)$$

For qualitative purposes, at low fractional conversion, J and the term $k/\sqrt{RT}$ can be replaced by their mean values J_m and k_m, respectively. The transformed rate equation is

$$\frac{G_0}{A(1+a)}\left(\frac{dX}{dz}\right)_{G_0} = J_m - k_m\sqrt{\frac{P \cdot J_m}{(1+a)}}\,X \quad (9)$$

Integrating over the reactor length and solving for the exit conversion yields

$$X_0 = \alpha\left(1 - \exp\left(-\frac{\beta V}{G_0}\right)\right) \quad (10)$$

where

$$\alpha = [J_m(1+a)/(P \cdot k_m^2)]^{1/2} \quad (11)$$

$$\beta = [k_m^2 \cdot J_m \cdot P \cdot (1+a)]^{1/2} \quad (12)$$

Equation (10) does not provide a simple means of data analysis because it cannot be graphically represented without a priori knowledge of J_m and k_m. Instead, we define an average percent conversion:

$$X_{\text{eff}} \equiv G_0\int_0^{1/G_0} X_0\, d\left(\frac{1}{G_0}\right) \quad (13)$$

This gives the simple linear relation

$$\frac{X_0 G_0}{1+a} = VJ_m - Vk_m\sqrt{\frac{PJ_m}{(1+a)}}\,X_{\text{eff}} \quad (14)$$

The average conversion X_{eff} can be determined from a graphical integration of conversion-inverse flow rate data. A plot of the molar rate of production of SO_2Cl_2, $G_0X_0/(1+a)$, versus effective conversion should be a straight line, with an intercept of J_mV, the total light absorbed, and a slope of $Vk_m \cdot \sqrt{PJ_m}/(1+a)$. Figure 2 shows the exit conversions for a typical set of experimental runs as a function of the inverse molar feed rate.

The values of X_{eff} were obtained by graphical integration, as indicated in Equation (13), for each experimental value of $1/G_0$. The corresponding plot of the rate of production of SO_2Cl_2 versus X_{eff} is shown in Figure 3. The straight line dependence indicates qualitative verification of the proposed rate law.

The effect of sulfur dioxide concentration was investigated by varying the partial pressure of SO_2 in the feed from 1/6 to 2/3 atmosphere with the partial pressure of Cl_2 held at 1/3 atmosphere, the remainder being argon. The data can be normalized by use of new variables defined by

$$X' = X_0/\sqrt{1+a} \quad (15)$$

$$G' = G_0/\sqrt{1+a} \quad (16)$$

$$X'_{\text{eff}} = X_{\text{eff}}/\sqrt{1+a} \quad (17)$$

Figure 4 shows the rates of production of SO_2Cl_2 as a function of the corresponding calculated values of X'_{eff}. Although there is a considerable amount of scatter in the data, there is no noticeable trend which can be correlated with the variation in SO_2 partial pressure.

The postulated rate law predicts there will be no effect of total pressure on either the forward or reverse reaction rates. Runs at 1, 1.5, and 2 atmospheres total pres-

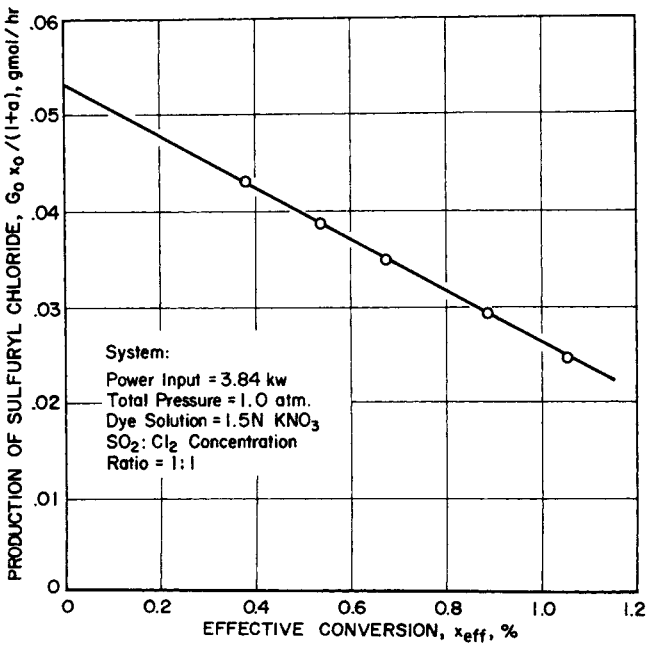

Fig. 3. Rate of production of sulfuryl chloride vs. effective conversion.

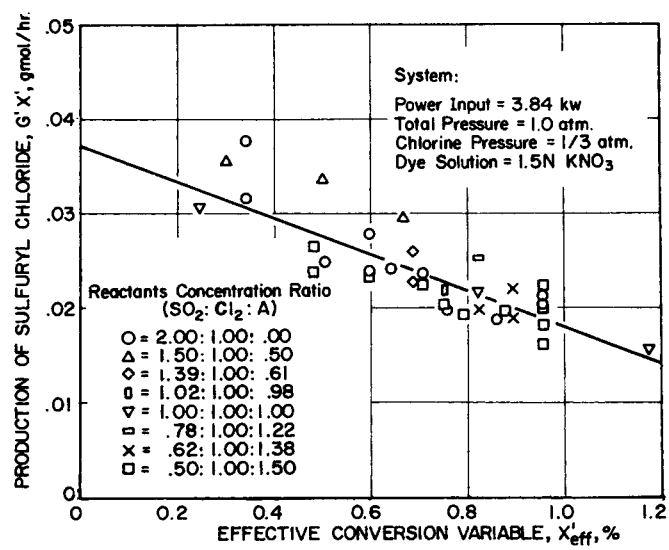

Fig. 4. Rate of production of sulfuryl chloride vs. effective conversion variable for several partial pressures of sulfur dioxide.

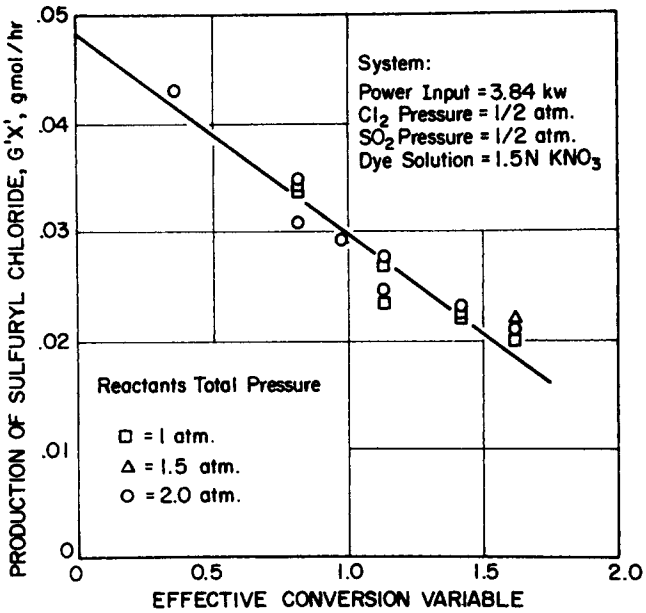

Fig. 5. Rate of production of sulfuryl chloride vs. effective conversion variable for several values of the total pressure.

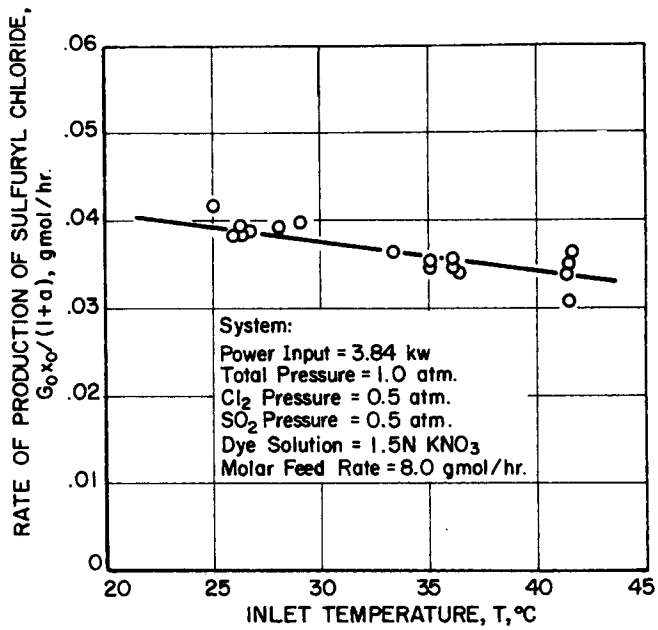

Fig. 6. Rate of production of sulfuryl chloride vs. temperature for a molar feed rate of 8.0 gmol/hr.

sure, with the partial pressures of both SO_2 and Cl_2 held at ½ atmospheres, support this postulate. The data can be normalized by using the relationships:

$$P_{SO_2} = P/(1 + a) \tag{18}$$

and

$$G'' = G_0/P \tag{19}$$

Data from several runs are depicted in Figure 5. These data can be adequately represented by a single curve, thus qualitatively eliminating any total pressure effects.

The effect of temperature on the rate of the forward reaction should be small if the postulated rate law is correct. Any effect should be due to thermal changes in light absorption properties. Two qualitative approaches were made to determine this effect.

First, a series of experimental runs was made in the temperature range 25 to 45°C using an equimolar feed mixture of sulfur dioxide and chlorine. The experimental observations are presented graphically in Figure 6. As shown, the reaction rate decreased approximately 0.9% per °C of temperature increase.

The second experimental approach is suggested by Equation (5). The initial, or forward, rate is given by the product $\alpha\beta$. At any given temperature, two runs suffice to determine α and β from Equation (5). A series of experiments at feed temperature of 15.4, 26.2, and 32.9°C gave the results shown in Figure 7. As shown, the forward rate decreases 0.7% per °C of temperature increase.

There are two factors to which the observed decrease in forward rate with increasing temperature can be attributed. First, according to the ideal gas law, the molar concentration of chlorine in the reactant mixture decreased approximately 0.35% per °C of temperature increase. Secondly, the extinction coefficients of both chlorine and potassium nitrate are functions of temperature. In qualitative terms, increasing the temperature of the potassium nitrate dye solution by 20°C shifts the cut-off region toward longer wavelengths by 20Å. Consideration of the spectral output of the light source indicates that this effect should decrease the rate at which light is absorbed by the reactants by approximately 0.25% per °C of temperature increase. Decreasing absorption by chlorine may be similarly estimated to cause the forward reaction to decrease by 0.1% per °C of temperature increase. The total predicted effect is a decrease of 0.7% per °C of temperature increase.

The effect of temperature on the reverse reaction rate should be contained in the rate constant k_m. Again, the parameters α and β can be used to determine this dependence. Assuming that k_m is an Arrhenius-type rate constant:

$$k_m = k_0 \exp^{(-E/RT)} \tag{20}$$

Then ratio β/α should exhibit temperature dependence involving an activation energy of $2E$:

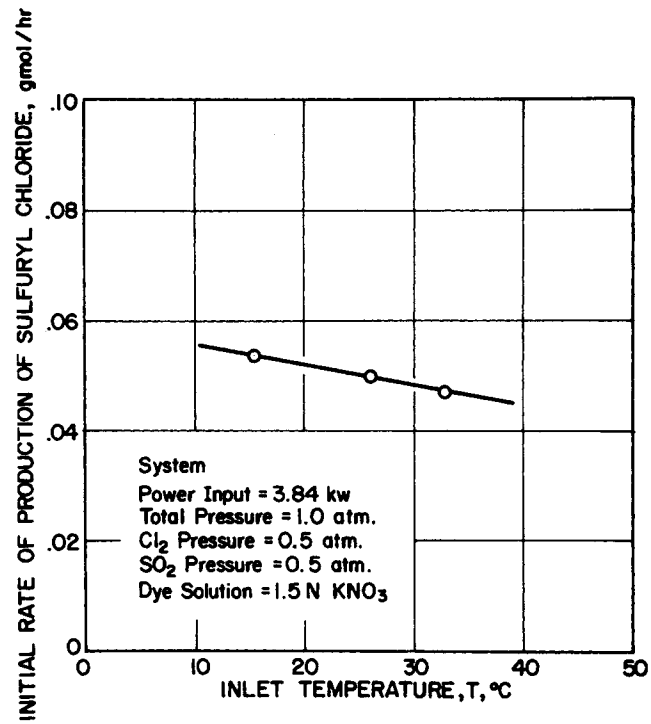

Fig. 7. Rate of the forward reaction as a function of inlet gas temperature.

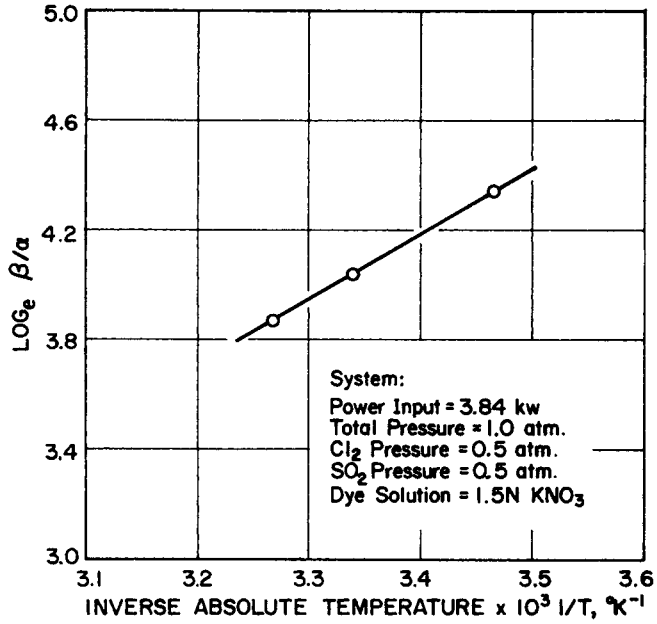

Fig. 8. Natural logarithm of β/α vs. the inverse of the absolute temperature.

$$\frac{\beta}{\alpha} = k_m^2 P = k_0^2 P \exp\left(-\frac{2E}{RT}\right) \qquad (21)$$

A plot of ln (β/α) versus $1/T$, as shown in Figure 8, should exhibit straight line dependence with a slope of $(-2E/R)$. The value of E computed from Figure 8 is -2.4 kcal/gmol. This is only an approximate value since feed temperature, not reaction temperature, was used.

In order to study the effect of the absorption of light by sulfur dioxide, the potassium nitrate solution was replaced by a 0.05 normal potassium iodide dye solution. Three series of runs were made with varying reactant mixture compositions while using potassium iodide dye solution.

The values of X_{eff} corresponding to each of the experimental points was calculated according to Equation (8). The rates of production of sulfuryl chloride for each of the three series of runs are presented as a function of the corresponding calculated values of X_{eff} in Figure 9. The extrapolated rates of production at zero conversion corresponding to the three concentration ratios were, respectively, 0.064, 0.076, and 0.084 gmol of sulfuryl chloride per hour. At low values of X_{eff} exhibit the expected linear relationship.

PROBABLE REACTION MECHANISM

The net observed photochemical reaction is a combination of one or more primary processes involving the absorption of quanta of radiation followed by one or more secondary thermal reactions involving the atoms, radicals and excited molecules generated by the primary processes.

A convenient starting point for modeling the photochemical reaction is a modified version of the reaction scheme suggested by Schumacher and Schott (1942). This scheme considers the reaction when only chlorine is involved in the primary process:

$$(1)\ Cl_2 + h\nu \rightarrow Cl\cdot + Cl\cdot$$

$$(1')\ Cl\cdot + Cl\cdot \xrightarrow{k_i[M]} Cl_2$$

$$(2) \text{ and } (2')\ SO_2 + Cl\cdot \underset{k_2'}{\overset{k_2}{\rightleftarrows}} SO_2Cl\cdot$$

$$(3)\ SO_2Cl\cdot + Cl\cdot \xrightarrow{k_3} SO_2Cl_2$$

$$(4)\ SO_2Cl_2 + Cl\cdot \xrightarrow{k_4} SO_2Cl\cdot + Cl_2$$

During this investigation, no effective third body for the recombination of chlorine was included in the reactant mixtures. This suggests that reaction (1′) was not significant, and thus may be deleted from any postulated reaction scheme.

Previous researchers have indicated that the quantum yield for the overall reaction is of the order of one. This indicates that the actual reaction scheme is of closed sequence, that is, does not involve a chain reaction. This means that the potential chain propagation reaction:

$$(4')\ SO_2Cl\cdot + Cl_2 \rightarrow SO_2Cl_2 + Cl\cdot$$

does not enter into the reaction scheme.

When sulfur dioxide enters into the primary process:

$$(5)\ SO_2 + h\nu \rightarrow SO_2^*$$

deactivation of the excited molecule can occur via one of several different routes:

$$(5')\ SO_2^* \rightarrow SO_2 + h\nu$$

$$(6)\ SO_2^* + M \rightarrow SO_2 + M$$

$$(7)\ SO_2^* + Cl_2 \rightarrow SO_2 + Cl\cdot + Cl\cdot$$

The fluorescence process described by reaction (5′) occurs with a natural radiative lifetime of 2×10^{-7} s, according to Calvert and Pitts (1966). At 25°C and 1 atm total pressure, a sulfur dioxide molecule undergoes approximately 250 collisions during this time span. If the collision process described by reactions (6) and (7) are at all efficient it will be anticipated that reaction (5′)

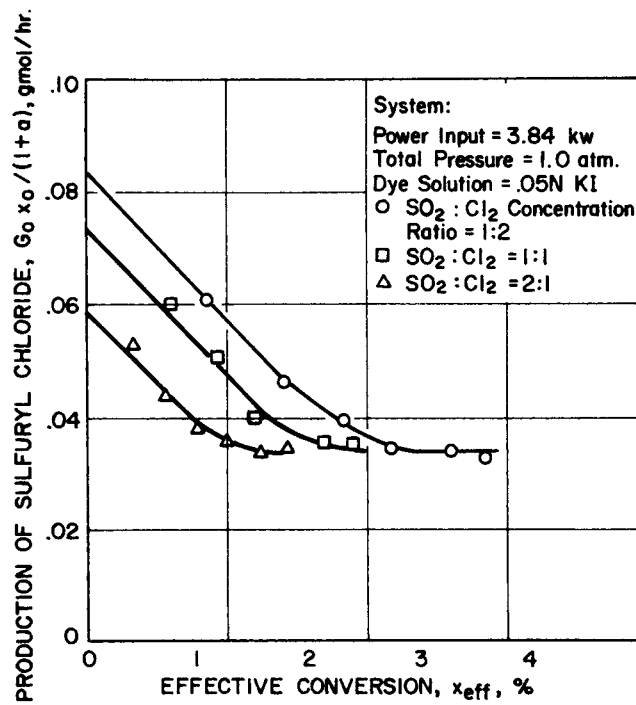

Fig. 9. Rate of production of sulfuryl chloride vs. effective conversion using KI dye solution.

does not enter into the actual reaction scheme.

If for the present it is assumed that reaction (7) predominates, the rate of generation of chlorine radicals is the sum of the rates of light absorption by chlorine and sulfur dioxide:

$$r_{Cl\cdot} = 2J_{Cl_2} + 2J_{SO_2} = 2J \tag{22}$$

where J is the total rate at which light is absorbed by the reactant mixture expressed in einsteins/liter-hr.

The rate of formation of sulfuryl chloride is the difference between the rate of reaction (3) and the rate of reaction (4):

$$r_{SO_2Cl_2} = k_3(SO_2Cl\cdot)(Cl\cdot) - k_4(SO_2Cl_2)(Cl\cdot) \tag{23}$$

Using the steady state hypothesis the rate of production of free radicals is equated to their rate of destruction:

$$2J = 2k_3(SO_2Cl\cdot)(Cl\cdot) \tag{24}$$

Making the further assumption that reactions (2) and (2′) are in thermal equilibrium

$$\frac{(SO_2Cl\cdot)}{(SO_2)(Cl\cdot)} = K_2 \tag{25}$$

the following rate expression can be written for the formation of sulfuryl chloride:

$$r_{SO_2Cl_2} = J - \frac{k_4}{(k_3K_2)^{1/2}}\sqrt{\frac{J}{(SO_2)}}(SO_2Cl_2) \tag{26}$$

The effective rate constant for the reverse reaction is $k_4/(k_3K_2)^{1/2}$. The effective activation energy for the reverse reaction is given by

$$E = E_4 - \frac{\Delta H_2}{2} - \frac{E_3}{2} \tag{27}$$

DISCUSSION

All of the parameter dependencies in the rate expression, (7), except for the J dependency of the reverse rate, were observed experimentally. The reverse rate was observed to be a function of the rate of light absorption; however, scatter in the experimental data made it impossible to differentiate between a half-power J dependency and some other J dependency, for example, a first power dependency.

There is both theoretical and experimental support for the half-power J dependence. In their investigation of the photochemical decomposition of sulfuryl chloride, Schumacher and Schott (1942) definitely observed that the reaction rate was proportional to $\sqrt{J}$. Theoretically all postulated mechanisms which led to a $\sqrt{(SO_2)}$ term in the denominator of the reverse rate also led to a $\sqrt{J}$ term in the numerator of the reverse rate.

The wall effect discussed by Schumacher and Schott (1942) is believed to be unimportant in this reactor. Noyes (1951) has considered the effect of wall terminations on photochemical reactions. He has shown that there is an effective thickness r_w over which the wall exerts an appreciable effect. This thickness is given by

$$r_w \cong 0.9\,D^{1/2}/(k_ik_{t2})^{1/4} \tag{28}$$

where D is the diffusion coefficient, k_i is the volumetric rate of initiation of radicals, and k_{t2} is the rate constant for homogeneous second order termination of radicals. For this study, r_w was approximately 0.002 cm, which is a negligible fraction of total reactor volume.

Schumacher and Schott (1942) experimentally observed an effective activation energy for the decomposition reaction of 18 kcal/gmol, but the effective activation energy observed during this investigation is − 2.6 kcal/gmol.

The most likely explanation for the anomaly is that in the present work the stationary state hypothesis was not entirely valid due to short residence times and high light intensities whereas in the work by Schumacher and Schott (1942) longer reaction times and lower light intensities met the necessary conditions for the application of the stationary state hypothesis.

Szabo et al. (1957, 1960) report that the thermal decomposition of sulfuryl chloride is described by a nonstationary state reaction mechanism. They report that there was a 0.9- to 12-min. induction period during which the stationary state assumption was not valid. The type, quality, and quantity of experimental data necessary to either prove or disprove this statement is beyond the scope of this investigation.

ACKNOWLEDGMENT

The authors express their sincere thanks to the National Science Foundation for financial support of this project.

NOTATION

a = ratio of feed concentration, less SO_2 concentration, to SO_2 concentration
a_i = stoichiometric coefficient
A = area, cm²
A_i = chemical species
$A(\lambda)$ = current output of photomultiplier, A
$\overline{A}$ = area per unit length, cm
b = feed ratio
c_p = heat capacity, cal/gmol K
C = concentration, gmol/liter
$\overline{c}$ = velocity of light, cm/s
d = optical path length, cm
D = diffusion coefficient, cm²/s
E = activation energy, kcal/gmol
$E(\lambda)$ = volumetric radiation emission rate, einstein/hr-cm³-Å
F_0 = molar feed rate, gmol/hr
G_0 = molar feed rate, gmol/hr
G' = feed rate variable (defined by Equation (16), Part II), gmol/hr
G'' = feed rate variable (defined by Equation (19), Part II), gmol/hr-atm
h = Planck's constant
H_c, H_I = spectrographic slit height, cm
ΔH_r = heat of reaction, kcal/gmol
$I(\lambda)$, $I'(\lambda)$ = intensity of radiation, einstein/hr-cm-Å
J = volumetric rate of light absorption, einstein/liter-hr
k_0 = pre-exponential rate constant, $s^{-1/2}$
k, k', k'', k_2, k_2', k_1', k_3, k_3', k_4 = rate constants
K = equilibrium constant
L = length, cm
M = spectrographic image magnification
P = pressure, atm
$Q(\lambda)$ = spectral radiance, einstein/hr-cm-Å-sr
r = radius, cm
r = reaction rate, gmol/liter-hr
r_w = effective thickness, cm
R = gas constant, cal/gmol°C or cm³atm/gmol K
R = radius, cm
$R(\lambda)$ = spectrographic calibration factor, einstein/hr-A-cm-Å-sr

S = area, cm^2
T = temperature, K or °C
u = molar average velocity, cm/s
U = heat transfer coefficient, kcal/cm^2 · s · K
V = reactor volume, liter
W = rate of internal heat generation, kcal/liter-hr
W_c, W_I = spectrographic slit width, cm
x = length along arc, cm
X = conversion, fraction
X_0 = exit conversion, percent or fraction
X' = conversion variable (defined by Equation (15), Part II), percent or fraction
Y = mole fraction
z = length along reactor, cm

Greek Letters

α = defined by Equation (11), Part II
β = defined by Equation (12), Part II
ϵ = molecular extinction coefficient, liter/gmol-cm
λ = wavelength, Å
ν = wave number, cm^{-1}
ϕ = angle, radians
Φ = quantum yield, gmol/einstein
ψ = light absorption function (defined by Equation (16), Part I)
θ = angle, radians

Subscripts

1 = outer radius
c = during calibration
eff = effective
i, j = species i or j
normal distance across reaction annulus
l = limiting reactant
m = mean value
0 = inlet to reactor
lower limiting value
inner radius
r = radial direction
s = surroundings
z = axial direction

LITERATURE CITED

Bonhoeffer, K. F., "Application of Quantum Theory to Photochemical Sensitizing," *Z. Phys.*, **13**, 94 (1923).

Calvert, J. G. and J. N. Pitts, *Photochemistry*, Wiley, New York (1966).

LeBlanc, M., K. Andrich, and W. Kangro, "Photochemische Umsetzungen im System $SO_2CL_2 \rightleftarrows SO_2 + Cl_2$ unter dem Einfluss von Strahlen Bestimmter Wellenlänge," *Z. Elektroch.*, **25**, 229 (1919).

Londergan, M. C., "The Photochemistry of the Formation of Sulfuryl Chloride," *Iowa State Coll. J. Sci.*, **17**, 95 (1942-43).

Noyes, R. M., "Wall Effects in Photochemically Induced Chain Reactions," *J. Am. Chem. Soc.*, **73**, 3039 (1951).

Schumacher, H. J., and C. Schott, "Die Photochemische Bildung von Sulfurylchlorid in der Gasphase aus Schwefeldioxyd und Chlor und sein durch Chlor Sensibilisierter Zerfall," *Z. Phys. Chem.*, **193**, 343 (1942-43).

Szabo, A. G., and T. Berces, "Der Mechanismus des Thermischen Zerfalls von Sulfurylchlorid," *Z. Phys. Chem.*, **12**, 168 (1957).

———., and P. Huhn, "Vollstandige Kinetische Analyse des Mechanismus des Thermischen Sulfurylchloridzerfalls," *ibid.*, **23**, 70 (1960).

Trautz, M., "Thermodynamics of Sulfuryl Chloride Equilibrium. IV. Velocity of the Reaction Approaching Equilibrium," *Z. Elektroch.*, **21**, 329 (1915).

Manuscript received July 16, 1973; revision received August 31 and accepted September 4, 1973.

Developing Pressure Profiles for Non-Newtonian Flow in an Annular Duct

A steady, laminar, isothermal flow of non-Newtonian fluids in the entrance region of an annulus has been studied experimentally. The axial pressure distributions, as well as the excess pressure energy, in the developing flow region are presented. The loss coefficients are found to increase with increasing flow behavior index for inelastic power law fluids. The experimental values of the loss coefficients are about 20% lower than those predicted from the boundary-layer approximation method presented earlier. A preliminary result indicates that the entrance loss for a viscoelastic fluid is much smaller than that for the inelastic fluid of the same flow behavior index.

SATINATH BHATTACHARYYA and CARLOS TIU

Department of Chemical Engineering
Monash University
Clayton, Victoria 3168, Australia

SCOPE

The problem of the developing flow of non-Newtonian fluids in the entrance region of an annulus is important because of its application in many polymer processing industries and in heat exchangers. Very little information concerning this area of research is available in the literature. When a fluid enters an annulus through a flow straightener followed by an abrupt contraction, it undergoes a change in the flow pattern from a reasonably flat velocity profile at the entrance to a fully-developed profile at a certain distance downstream. The change in the velocity causes an increase in the fluid kinetic energy and an increase in viscous friction associated with a loss in pressure energy which is larger than that experienced in the fully developed region. The object of the present study is to determine experimentally the axial pressure distribution for the developing flow of non-Newtonian fluids in the entrance region of an annular duct, thus providing a measure of the excess pressure losses in the entrance region. The experimental results will also serve to justify the theoretical analyses presented by the authors (1973) in an earlier paper.